Application of polycapillary x ray lens to eliminate both the effect of x ray source size and scatter of the sample in laboratory tomography

Xuepeng Sun (孙学鹏)[1,2,3], Zhiguo Liu (刘志国)[1,2,3], Tianxi Sun (孙天希)[1,2,3,*], Longtao Yi (易龙涛)[1,2,3], Weiyuan Sun (孙蔚渊)[1,2,3], Fangzuo Li (李坊佐)[1,2,3], Bowen Jiang (姜博文)[1,2,3], Yongzhong Ma (马永忠)[4], and Xunliang Ding (丁训良)[1,2,3]

[1]*The Key Laboratory of Beam Technology and Materials Modification of the Ministry of Education, Beijing Normal University, Beijing 100875, China*

[2]*College of Nuclear Science and Technology, Beijing Normal University, Beijing 100875, China*

[3]*Beijing Radiation Center, Beijing 100875, China*

[4]*Center for Disease Control and Prevention of Beijing, Beijing 100013, China*

**Corresponding author: stx@bnu.edu.cn*

Received April 11, 2015; accepted July 9, 2015; posted online August 4, 2015

A tomography device based on a conventional laboratory x ray source, polycapillary parallel x ray lens (PPXRL), and polycapillary collimating x ray lens (PCXRL) is designed. The PPXRL can collect the divergent x ray beam from the source and focus it into a quasi-parallel x ray beam with a divergence of 4.7 mrad. In the center of quasi-parallel x ray beam, there is a plateau region with an average gain in power density of 13.8 and a diameter of 630 μm. The contrast of the image can be improved from 28.9% to 56.0% after adding the PCXRL between the sample and the detector.

OCIS codes: 340.0340, 220.0220.
doi: 10.3788/COL201513.093401.

Tomography is a nondestructive testing technology, and it has wide applications in the fields of industrial inspection, safety inspection, medical diagnosis, and so on[1–6]. Tomography works on different x ray absorption efficiencies of different parts of an object. In order to obtain an x ray image with a high spatial resolution, the conventional x ray source with a micro focus is often used. Such a micro focused x ray source is helpful in decreasing the blurring effect from the source size on the image because such blurring increases with the increasing source size[7]. The x ray image can be magnified with the divergent beam from a micro-focused x ray source, which decreases the requirement that the detector have a high spatial resolution. However, the power of such a micro-focused x ray source is so low that it affects the efficiency of the x ray imaging. A quasi-parallel x ray beam plays an important role in tomography because the small radiation divergence of the quasi-parallel x ray beam results in a small blurring effect and the high resolution of the x ray image. Therefore, quasi-parallel synchrotron radiation is an ideal source for tomography with high quality. However, the synchrotron radiation facility is so large and expensive that it is not available to a conventional laboratory. In order to obtain a quasi-parallel x ray beam from a conventional x ray tube for desktop x ray tomography of low-contrast samples, a polycapillary parallel x ray lens (PPXRL) is used to focus the divergent x ray beam from the x ray tube into a quasi-parallel beam with a residual divergence of several milliradians[8]. There are some methods of decreasing the effect of x rays scattered by the sample on the x ray image. The anti-scatter grids and air gaps are the most common methods for reducing the scatter, but both have limitations. The anti-scatter grids suffer from their inefficient use of the x ray source. Therefore, cone-shaped polycapillary x ray optics are designed to be used as to prevent scattering for the efficient use of the divergent x ray beam from the source[9]. As for the air gap, the large distance between the sample and x ray imaging detector results in the decayed incident x ray beam and low imaging efficiency.

In this Letter, in order to decrease the effect the large source size has on the image quality, we designed a PPXRL to focus the divergent x ray beam from a laboratory Mo target x ray source with a source size of hundreds of microns into a quasi-parallel beam for tomography. As opposed to using the desktop x ray tomography for low-contrast samples with only a PPXRL that was used in [8], a cylindrical polycapillary collimating x ray lens (PCXRL) was designed and placed between the sample and the detector in order to decrease the effect of the x rays scattered from the sample on the image quality. Compared with the conventional multi-hole collimators and multi-hole anti-scatter devices, both the PPXRL and PCXRL work on total external reflection, and accordingly could be used for the efficient use of the x ray source. Therefore, the PPXRL and PCXRL can not only decrease the effects from the source size and the scattered x rays, respectively, but they can also improve the imaging efficiency. In this Letter, the properties of laboratory tomography based on PPXRL, PCXRL, and a large-focus x ray source were studied.

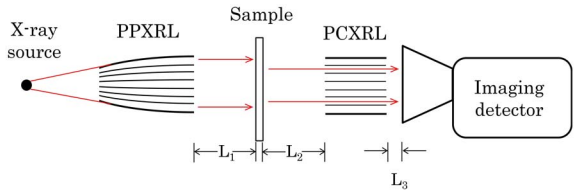

Fig. 1. Scheme of the x ray absorption imaging device based on a polycapillary x ray lens.

The scheme of the tomography device based on the polycapillary x ray lens is shown in Fig. 1. The x ray source is a Mo rotating anode x ray generator (RIGAKU RU-200, 60 kV–200 mA) whose spot size is 300 μm × 300 μm. The cell size of the x ray image system is 6.5 μm× 6.5 μm. When the PPXRL and PCXRL were produced by hundreds of thousands of borosilicate glass fibers, they were all taken from the same monolithic polycapillary x ray lens. Figure 2 shows a picture of the PPXRL and PCXRL used in the experiment, and the cross section of the outside of the PPXRL, which indicates that the channel size of the PPXRL is about 7 μm. Table 1 shows the main geometric parameters of the PCXRL and PPXRL. In the experiment, the sample, PCXRL, and PPXRL were adjusted using a five-dimensional stage with mini step size of 1 μm.

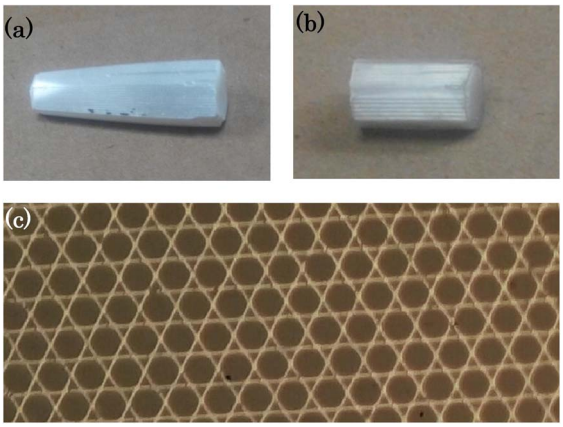

Fig. 2. (a) Picture of the PPXRL. (b) Picture of the PCXRL. (c) Cross section of the outside of the PPXRL. The channel size is about 7 μm.

Table 1. The Main Geometric Parameters of the PPXRL and PCXRL

Parameter	PPXRL	PCXRL
Length/mm	73.2	43.7
Input Diameter/mm	3.7	4.3
Output Diameter/mm	4.3	4.3
Input Focal Distance/mm	71.2	Not available
Number of the Capillary/ca	320000	320000

We characterized the polycapillary x ray lens with a CCD detector. The x ray source worked at 20 kV and 10 mA. Figure 3 shows the photograph of the output beam of the PPXRL captured by the CCD detector at 30 cm from the output of the PPXRL. The output beam size, which is the full width at half maximum (FWHM) of the intensity distribution curve of the output beam, is 1700 μm. The intensity distribution curve used to measure the size of the output beam of the PPXRL is shown in Fig. 4. The curve of the intensity of the beam cross section of the PPXRL is a Gaussian distribution. The reason for this is that the length and curvature of the fibers near the edge of the PPXRL are bigger than that of those in the center. Thus, the throughput of the fibers near the edge of the PPXRL was lower than that of those in the center[10,11]. Similarly, a series of sizes of output beams of the PPXRL with the CCD situated in different places can be obtained, and the divergence of the beam of the PPXRL was accordingly calculated to be 4.7 mrad by the method in Ref. [12]. The gain in power density of the PPXRL (G) is the ratio of x ray intensity with and without the PPXRL at some point of space. Thus, the gain of the PPXRL can be represented as

$$G = \frac{I_{\text{lens}}}{I_o}, \tag{1}$$

where I_{lens} is the x ray intensity with the PPXRL, and I_o is the x ray intensity without the PPXRL at the same point. When the PPXRL was removed, and the position of x ray source and the CCD remained unchanged, the x ray intensity distribution without the PPXRL could be acquired. The distribution of the gain of the PPXRL in the cross

Fig. 3. Image of output beam of PPXRL at the distance of 30 cm from the CCD detector.

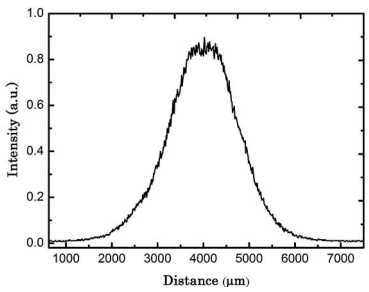

Fig. 4. X ray intensity distribution of the output beam of the PPXRL at a distance of 30 cm from the CCD detector.

section of the output beam of the PPXRL is shown in Fig. 5, which was figured by counting each pixel of the picture captured by the CCD with and without the PPXRL. In the region of the FWHM of the output beam of the PPXRL, the gain of the PPXRL ranges from 6.7 to 14.1. The high gain power density of the output beam of the PPXRL can shorten the imaging time. In the gain curve, there was a rounded plateau region with a diameter of approximately 630 μm and an average gain of about 13.8, which corresponded to the central part of the output beam of the PPXRL. This plateau region with a high power density is helpful in analyzing a micro object smaller than the focal spot of the polycapillary optics[13]. The transmission efficiency of the PCXRL is about 60% for the quasi-parallel x ray beam from the PPXRL, because almost all of the quasi-parallel x ray beam spreading from PPXRL can go through the PCXRL, and only the walls of a capillary can partially stop the spread of the x rays.

We characterized the imaging performances of the tomography equipment based on the PPXRL and PCXRL by a mesh made of stainless steel wires (see Fig. 6). The exposure time of the CCD detector was 1 s. The distance from the PPXRL to the mesh (see Fig. 1) is 20 cm. The distance from the mesh to the input side of the PCXRL is 2 cm (see Fig. 1). The distance from the output side of the PCXRL to the CCD detector is 2 cm (see Fig. 1). Figures 7(a) and 7(b) were the images of the mesh captured by the device as shown in Fig. 1 with and without the PCXRL. The intensity profile through the image of the Figs. 7(a) and 7(b) is shown in Figs. 8(a) and 8(b), in which the red curve is the intensity profile without the sample. The image sharpness can be characterized by the contrast (C) of the image, which was defined as[14]

$$C = \frac{I_{\max} - I_{\min}}{I_{\max} + I_{\min}}. \tag{2}$$

The intensities $I_{\max}$ and $I_{\min}$ can be taken from the intensity profile of the sample, as shown in Fig. 8. As shown in Fig. 8, the contrast of the images of the mesh increased from 28.9% to 56.0% when the PCXRL was used as an anti-scatter. The reason for this is that when the PPXRL and PCXRL were aligned as shown in the Fig. 1, the scattered x rays from the sample, which had scattered angles larger than the total reflection angle for the inner wall of the PCXRL, cannot get through the PCXRL. Due to the non-uniform original intensity, which is indicated in Fig. 8 by the red line, the mesh image captured by the designed tomography device could only show a part where the x ray intensity has high gain. So in order to eliminate this influence, we take the flat-field correction by dividing the x ray intensities with the sample by the intensities without the sample. As shown in Fig. 9, after this processing, the intensity profile became more even [see Fig. 9(a)], and the image of the mesh not only became more uniform, but can also display a broad field [see Fig. 9(b)].

In order to study the contrast loss in the image due to the geometrical blur from the divergence of the quasi-parallel beam from the polycapillary x ray lens, we have

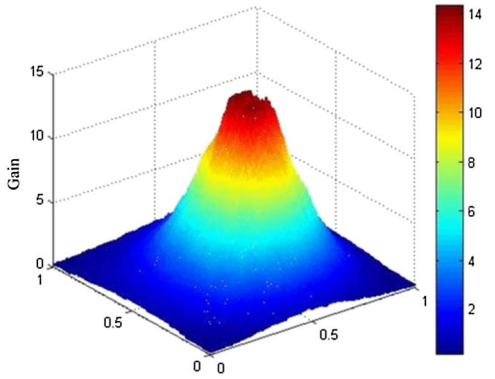

Fig. 5. Distribution of the gain of the PPXRL at a distance of 30 cm from the CCD detector.

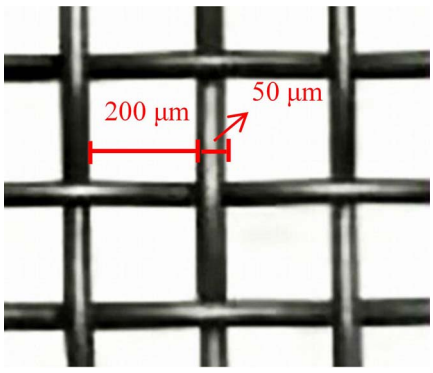

Fig. 6. Picture of the mesh used in the experiment.

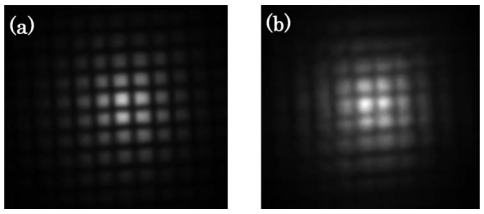

Fig. 7. Image of the mesh at a distance of 20 cm from the PPXRL taken by the tomography device (a) with and (b) without the PCXRL.

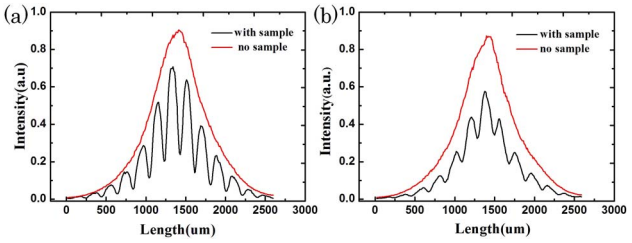

Fig. 8. Corresponding intensity profiles of the images in Fig. 7(a) and 7(b).

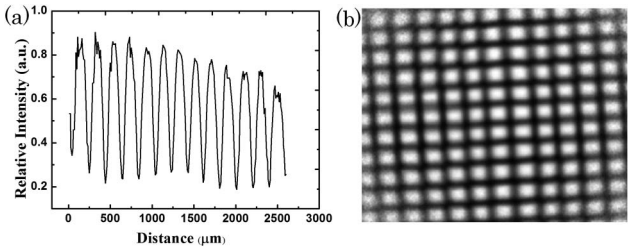

Fig. 9. (a) Ratio of intensities in Fig. 8. (b) Image of Fig. 7 after flat-field correction.

taken a series of images of the mesh in different locations (see Fig. 10). Images 1, 2, 3, and 4 of the mesh shown in Fig. 10(a) were captured at $L_3 = 2$, 8, 14, and 20 cm, respectively, with $L_1 = 20$ cm and $L_2 = 2$ cm (see Fig. 1). Similarly, Fig. 10(b) shows the mesh images at $L_2 = 2$, 8, 14, and 20 cm, respectively, with $L_1 = 20$ cm and $L_3 = 2$ cm (see Fig. 1). As shown in Fig. 10, the images of the mesh become increasingly blurred with the larger distances in both cases, and the corresponding decrease of their contrasts is shown in Fig. 11. The divergence of the polycapillary x ray lens in the PPXRL and the PCXRL had two components: the divergence from the fiber-to-fiber misalignment (global divergence) and the divergence of individual capillaries (local divergence), which mainly

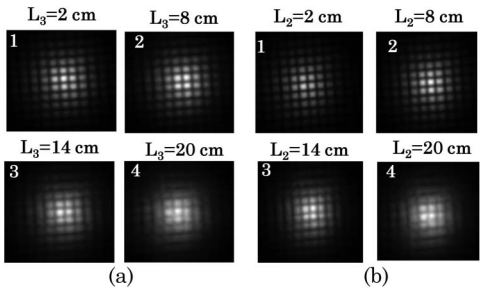

Fig. 10. Image of the mesh in different places. (a) $L_1 = 20$ cm and $L_2 = 2$ cm. (b) $L_1 = 20$ cm and $L_3 = 2$ cm.

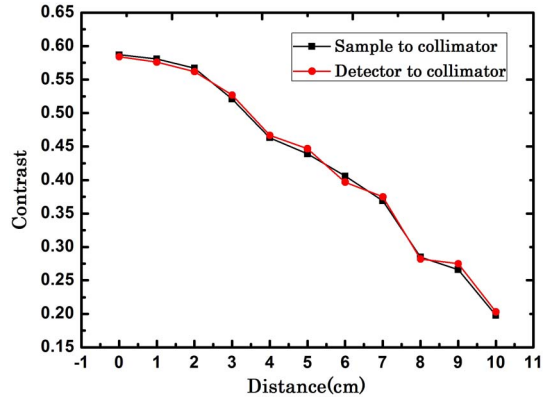

Fig. 11. Contrast of the images as a function of the distance between the detector and the outside of PCXRL (the red line), and between the sample and the inside of PCXRL (the black line).

depends on the critical angle of total reflection of the x rays from the internal capillary wall[15,16]. Figure 12 shows the distribution of the local angular divergence of the output beam from the PPXRL by scanning an aperture with a size of 50 μm across the end fact of the PPXRL and measuring the angular divergence for each position of this aperture. This curve indicates that the angular divergence of the fibers in the edge of the end face of the PPXRL is bigger than that of those in the center. This is mainly caused by the face that it is easier to misalign the fibers in the edge of the end face of the PPXRL. The image contrast decreased with the increasing distances between the PCXRL and the detector. The reason for this is that the blurring effect is in direct proportion to the distance between the PCXRL and the detector for the PPXRL with a given divergence[8]. This was also the reason for the decrease of the contrast with increasing distances between the sample and the PCXRL.

The change of the contrast of the mesh with the distances of L_2 and L_3 has the same trend. Therefore, to acquire an image with a high contrast, the sample and the detector should be placed close to the input and output side of the PCXRL, respectively.

In the designed tomography device based on the polycapillary x ray lens, the divergent x ray emitting from the conventional large-focus x ray source can be transformed into a quasi-parallel beam with a beam divergence of several milliradians. This quasi-parallel beam has hardly any relationship with the source size and shape, and is helpful in reducing the effect of the large source size on the image quality. Moreover, compared with the quasi-parallel beam acquired by pinhole collimators or Soller slits, which sacrifice part of the intensity of the incident beam, the quasi-parallel beam from the PPXRL has a high gain in the power density that can effectively reduce the measurement time of the proposed setup in this Letter. As shown in Fig. 5, the average gain of the power density of the PPXRL is about 10, and this indicates that the

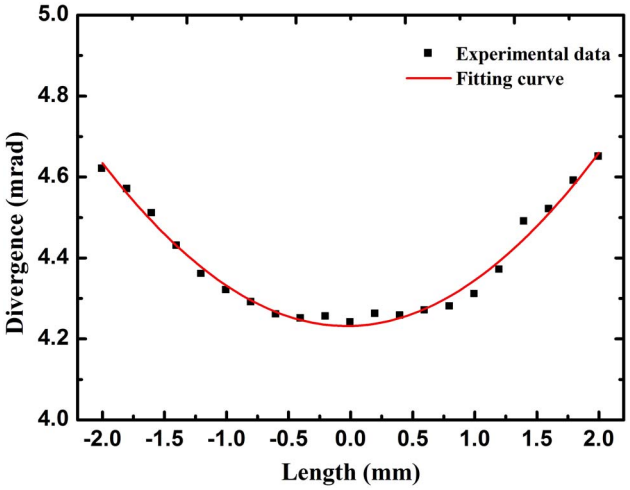

Fig. 12. Distribution of the local angular divergence of the output beam from the PPXRL.

measurement time of the proposed setup could be reduced theoretically to less than 1/10 of the measurement time of a setup with pinhole collimators or Soller slits. Additionally, because the PCXRL and PPXRL were from the same monolithic polycapillary x ray lens, the PCXRL working as an anti-scatter can not only allow an efficient use of the quasi-parallel x ray beam from the PPXRL, but it also heavily reduces the effect of the x rays scattered from the sample and improves the contrast of the image.

In conclusion, we design a PPXRL and PCXRL for the tomography with a laboratory-appropriate, large-focus x ray source, and characterized their imaging properties with a stainless steel wire mesh. The experimental results show that the tomography device based on the PPXRL and PCXRL can not only transform the divergent x ray beam into a quasi-parallel beam for imaging by eliminating the influence of the penumbra effect from the source size, but they also reduce the scatter from the sample, which results in the improvement of the image contrast. Moreover, the high gain in the power density of the PPXRL can increase the imaging efficiency. Thus, a tomography device based on an x ray source that is commonly found in the laboratory and on the PPXRL and PCXRL has potential applications in many fields, such as materials science and medicine, and so forth.

This work was supported by the National Natural Science Foundation of China (No. 11375027) and the Fundamental Research Funds for the Central Universities (No. 2014kJJCA03).

REFERENCES

1. V. C. Tidwell, L. C. Meigs, T. Christian-Frear, and C. M. Boney, J. Contam. Hydrol. **42**, 285 (2000).
2. D. Kim, S. Park, J. H. Lee, Y. Y. Jeong, and S. Jon, J. Am. Chem. Soc. **129**, 7661 (2007).
3. K. Ueta, K. Tani, and T. Kato, Eng. Geol. **56**, 197 (2000).
4. J. Qi, Y. Ren, G. Du, R. Chen, Y. Wang, Y. He, and T. Xiao, Acta Opt. Sin. **33**, 104001 (2013).
5. S. Yi, B. Mu, X. Wang, J. Zhu, L. Jing, Z. Wang, and P. He, Chin. Opt. Lett. **12**, 013401 (2014).
6. T. Xiao, H. Xie, B. Deng, G. Du, and R. Cheng, Acta Opt. Sin. **34**, 0100001 (2014).
7. T. Sun and C. A. MacDonald, J. X ray. Sci. Technol. **23**, 141 (2015).
8. D. Hampai, L. Marchitto, S. B. Dabagov, L. Allocca, S. Alfuso, and L. Innocenti, Nucl. Instrum. Meth. B. **309**, 264 (2013).
9. D. G. Kruger, C. C. Abreu, E. G. Hendee, A. Kocharian, W. W. Peppler, C. A. Mistretta, and C. A. MacDonald, Med. Phys. **23**, 187 (1996).
10. V. A. Arkad'ev, A. I. Kolomitsev, M. A. Kumakhov, I. Y. Ponomarev, I. A. Khodeev, Y. P. Chertov, and I. M. Shakhparonov, Usp. Fiz. Nauk. **157**, 529 (1989).
11. J. B. Ullrich, V. Kovantsev, and C. A. MacDonald, J. Appl. Phys. **74**, 5933 (1993).
12. T. Sun and X. Ding, J. Appl. Phys. **97**, 124904 (2005).
13. T. Sun, Z. Liu, Y. Li, G. Wang, G. Zhu, Q. Xu, Y. Ma, X. Lin, H. Liu, P. Luo, Q. Pan, Y. Teng, and X. Ding, Nucl. Instrum. Meth. B **268**, 3554 (2010).
14. T. Sun and C. A. MacDonald, J. Appl. Phys. **113**, 053104 (2013).
15. T. Sun, Z. Liu, Y. Li, X. Lin, P. Luo, Q. Pan, and X. Ding, Nucl. Instrum. Meth. B **269**, 2758 (2011).
16. C. A. MacDonald, J. X ray Sci. Tech. **6**, 32 (1996).